

Article

A Probabilistic Model for Minimization of Solar Energy Operation Costs as Well as CO₂ Emissions in a Multi-Carrier Microgrid (MCMG)

Hassan Ranjbarzadeh¹, Seyed Masoud Moghaddas Tafreshi², Mohd Hasan Ali³ , Abbas Z. Kouzani¹ 
and Suiyang Khoo^{1,*}

¹ School of Engineering, Deakin University, Geelong, VIC 3216, Australia; hranjbar@deakin.edu.au (H.R.); abbas.kouzani@deakin.edu.au (A.Z.K.)

² Electrical Engineering Department, University of Guilan, Rasht P.O. Box 1841, Iran; tafreshi@guilan.ac.ir

³ Electrical and Computer Engineering Department, University of Memphis, Memphis, TN 38152, USA; mhali@memphis.edu

* Correspondence: sykhoo@deakin.edu.au

Abstract: This paper proposes a probabilistic model with the aim to reduce the solar energy operation cost and CO₂ emissions of a multi-carrier microgrid. The MCMG in this study includes various elements such as combined heat and power (CHP), electrical heat pump (EHP), absorption chiller, solar panels, and thermal and electrical storages. A MILP model is proposed to manage the commitment of energy producers, energy storage equipment, the amount of selling/buying of energy with the upstream network, and the energy consumption of the responsible electrical loads for the day-ahead optimal operation of this microgrid. The proposed operation model is formulated as a multi-objective optimization model based on two environmental and economic objectives, using a weighted sum technique and a fuzzy satisfying approach. In this paper, the 2 m + 1-point estimate strategy has been used to model the uncertainties caused by the output power of solar panels and the upstream power supply price. In order to evaluate the performance of the proposed model, and also for minimizing cost and CO₂ emissions, the simulation was conducted on two typical cold and hot days. Numerical results show the proposed model's performance and the effect of electrifying the heating and cooling of the microgrid through the EHP unit on greenhouse gas emissions in the scenarios considered.

Keywords: residential energy hub; responsive equipment; multi-objective optimization; point estimate method; EHP; weighted sum technique; fuzzy



Citation: Ranjbarzadeh, H.; Tafreshi, S.M.M.; Ali, M.H.; Kouzani, A.Z.; Khoo, S. A Probabilistic Model for Minimization of Solar Energy Operation Costs as Well as CO₂ Emissions in a Multi-Carrier Microgrid (MCMG). *Energies* **2022**, *15*, 3088. <https://doi.org/10.3390/en15093088>

Academic Editor: Luis Hernández-Callejo

Received: 29 June 2021

Accepted: 27 March 2022

Published: 23 April 2022

Publisher's Note: MDPI stays neutral with regard to jurisdictional claims in published maps and institutional affiliations.



Copyright: © 2022 by the authors. Licensee MDPI, Basel, Switzerland. This article is an open access article distributed under the terms and conditions of the Creative Commons Attribution (CC BY) license (<https://creativecommons.org/licenses/by/4.0/>).

1. Introduction

The cost of energy and air pollution reduction are very important issues for the global community, since there has been a significant decrease in the amount of fossil fuels and a rise in global warming over the last decades [1]. With the growing dominance of smart grids and rapid advances in information and communication technologies (ICT) there has been a rapid evolution in smart grid [2–5] microgrids [6,7], resulting in a significant decrease in energy costs and providing more profit to the community of consumers in residential and commercial properties.

In line with the establishment of networks for natural and considerable benefits of this energy carrier, the popularity of the CHP technology has also increased significantly [1,2]. The CHP technology provides the ability to harness multiple energy carriers using energy hubs to meet the demands in microgrids. Around half of the global energy consumption is for the purpose of heating. As outlined in the report published by the International Energy Agency (IEA) in 2009, 47% of global consumption of energy is for providing heat, 27% is dedicated to transportation, 17% is for supplying electricity, and 9% is considered as non-energy usages.

Electric heating and cooling can be considered a good choice to decrease the emitted carbon and address the needs for providing heating and cooling inside buildings, which would subsequently lead to a reduction in the usage of fossil fuels. In this context, EHP can be considered as a crucial technology to accomplish a significant decrease in the use of fossil fuels [8].

The aim of this study is to adopt a probabilistic optimization method in order to develop a structured hub model for a microgrid based on the energy flow between its components. The proposed hub is not only able to respond to the total electrical, cooling, and thermal demand, but it can also provide the ability to sell electricity to the service provider of the upstream network. The constituent components of the developed hub are solar panels, EHP, CHP, absorption chiller, responsive loads, and thermal and cooling storages for heating and cooling. In addition, uncertainties associated with the electricity price and the power output from the solar panels are taken into consideration. These uncertainties are covered by the 2 m + 1-point estimation approach. Using a weighted sum technique and fuzzy logic, environmental (minimizing CO₂ emissions) and economic (minimizing energy cost) objectives are considered in a multi-objective formula in order to schedule both the energy hub operation and the energy consumption of the responsible electrical equipment of the hub. Since the two objectives of minimizing costs and CO₂ emissions are contradictory, the Pareto curves for costs and CO₂ emissions show a trade-off between these two conflicting objectives. With the above points in mind, the next section provides a review of the literature relevant to this study. This is followed by the presentation of an overall structure of the developed energy hub model in Section 3. Section 4 provides the mathematical model that is adopted by the energy hub, including objective functions, and operating and system constraints. In Section 5, the numerical results from the implementation of the proposed hub model are presented. Finally, the paper concludes with the main findings of this study and recommendations for future research.

2. Literature Review

The energy hub model for a smart home is presented in Ref. [2]. A residential CHP cogeneration technology and a plug-in hybrid electric vehicle are employed in the model. The output of the hub has different thermal and electrical loads, and the objective of short-term energy hub planning is minimizing energy costs. The simulation results of this paper demonstrate that by applying home load management (HLM), electrical demands shift to low-tariff times and the cost of paying for energy decreases. In Ref. [9], a new framework for microgrid energy management in the context of a renewable-based residential energy hub is proposed. The main technique used is based on probabilistic optimization. Ref. [10] has proposed an energy hub in the electrical distribution network that has a variety of energy carriers such as gas, electricity, wind, and water at its input, and supplies electricity, gas, heat, and water at its output. The proposed energy hub is optimized based on the objective function that considers economic aspects, greenhouse gas emissions, reliability in a randomized and predicted region of wind, electricity demand, and real time market pricing. In this paper, a Monte Carlo simulation is used to generate real time pricing, wind speed, and predicted electrical demand. Ref. [11] performed an optimal 24 h scheduling of an energy hub. The energy hub includes renewable energy resources, thermal and electrical storages, and demand response. The optimal operation of the energy hub is aimed at reducing the cost of purchasing electricity and gas and reducing the cost of limiting demand. It also earned revenue through the sale of thermal and electrical loads and plans energy consumption in a smart home using a microgrid system. In Ref. [1] a mixed integer linear programming (MILP) model is proposed to schedule the energy consumption within a smart home using a microgrid system. The daily power consumption tasks are scheduled by coupling environmental and economic sustainability in a multi-objective optimization using the epsilon-constraint method. In Ref. [12] a smart grid energy management model is presented in which electrical and thermal appliances are jointly scheduled. The proposed method aims at minimizing the electricity cost of a residential

customer by scheduling various type of appliances through considering the resident's consumption behavior, seasonal probability, social random factor, discomfort index, and appliances starting probability functions.

Ref. [5] reviews strategies for controlling microgrids networks with an energy storage system. This paper presents a comprehensive review of decentralized, centralized, multi-agent, and intelligent control strategies that have been proposed to control and manage distributed energy storage. In this paper, the authors also demonstrate the potential range of services that can be provided by these storages, their control complications, and proposed solutions. Refs. [4,13] propose a new energy management system of networked microgrids and a cost-optimized microgrid using Bayesian reinforcement learning, respectively. In Ref. [13], a day-ahead self-healing scheduling approach in isolated networked microgrid systems is proposed. The proposed approach is based on a two-level flexible energy management system (EMS). Ref. [5] addresses the energy trading problem among microgrids. The authors mainly apply the Bayesian coalitional reinforcement learning-based model by forming stable coalitions to minimize the cost of microgrids.

Ref. [14] provides a new method for modeling energy hubs based on the energy flow between its constituent elements. The modeling of the energy hubs with various and interconnected elements is facilitated using this method. This paper proposes a MILP model for 24 h short-term planning, the objective of which is to provide the total thermal, cooling, and electrical demands of an assumptive building with maximum profit. Additionally, in the proposed hub modeling, the possible operation region for the CHP system is associated with the technical constraints of the hub energy equipment. Ref. [15] is a way to integrate distributed energy systems on a local scale. The proposed method is based on the concept of an energy hub that manages the relationship between the input and output of energy flows, and therefore, optimizing energy consumption.

The proposed hub includes a photovoltaic system, biomass, a small hydroelectric power generator with local thermal systems, local converters, and local storage technology. The proposed method reduces the peak energy demand of neighbors on the network and reduces energy costs. Ref. [16] is a complex model of an energy hub under different scenarios modeled and optimized in order to minimize both cost and greenhouse gas emissions. Hubs are connected to each other through different distribution networks and are characterized by specific thermal and electrical profiles. The input energy of each hub in the grid is supplied from the main grid, natural gas, hydrogen, renewable resources, or the output of other energy hubs inside the grid. In this paper a multi-objective function is considered to optimize cost and emission reduction.

Ref. [17] suggests an automatic residential partnership framework that minimizes the cost of energy consumption of a smart grid. In this paper, the incentive-based and price-based tariffs are considered by retailers for consumers, and the objective function is to minimize the cost of energy and discomfort for consumers. The decision variables of this paper are the operation modes of the responsive equipment and the charging and discharging cycles of battery storage and hybrid electric vehicles. Ref. [18] extends the existing demand response (DR) programs to the integrated demand response (IDR) programs with the aim of modifying both electricity and natural gas consumption on the customer side. The research problem is formulated as a non-cooperative game problem. The main goal is to maximize the profit of natural gas and electricity utility companies and minimize the cost of customers' consumption. Ref. [19] has proposed a new method for optimal electric distribution system expansion planning (OEDSEP) using the concept of an energy hub. The proposed approach uses the energy hub model to evaluate the effects of multi-carrier energy systems on the OEDSEP. In this paper, the objective is to minimize the operation costs and investment, while increasing the reliability of the system. Ref. [20] has expanded mid-term energy hub management through restructured power systems. The main feature of this paper is the representation of a new model for mid-term energy hub management, taking into account risks in the proposed method and through considering the uncertainty in the pool-based market and bilateral contracts, and the power output of

the PV systems in the mid-term energy hub management. The pool-based market, bilateral contracts, and wind speed are predicted using an auto regressive integrated moving average (ARIMA) and an auto regressive moving average (ARMA) time series respectively. Ref. [21] has analyzed the optimal power flow problems of multi-carrier energy networks in the presence of interconnected energy hubs. They provided a multi-objective model that minimizes energy costs, and electricity and natural gas losses for the reliable operation of the energy networks. They have also evaluated the impacts of networked energy hubs on the power systems.

Despite the research on improving both the minimization of solar energy operation costs and reducing CO₂ emissions in a multi-carrier microgrid, the number of related research reports remains limited to date. Considering the above absences, the aim and the innovative aspect of the present study and the contributions may be summarized as follows:

1-A new probabilistic optimization method is utilized for developing a microgrid energy hub including 7 components by considering the flow of energy between their hub components.

2-Two optimization objectives are considered to operate the energy hub as well as the commercial and industrial electrical load.

3-The constraints limiting the possible values of an energy hub including 7 components for the decision variables in the optimization model are defined.

3. Energy Hub and Mathematical Model

The hub structure suggested in this study is represented in Figure 1. Electricity and natural gas networks provided the input for this hub. The hub output was comprised of constant and responsive electrical loads, and thermal and cooling loads. The proposed hub structure included solar panels, which are renewable resources, CHP and EHP converters, and absorption chillers, as well as devices for storing electricity and heat. The natural gas was fed into the CHP unit which produced both heat and electricity concurrently. The electrical energy was consumed by the EHP unit to relocate the heat from an environment with a relatively cool temperature to another environment with a warm temperature. The thermal energy was then fed into the absorption chiller, which subsequently created cold air. At the final step, the charge and discharge of electricity was conducted using the electrical and thermal storage devices.

According to the energy flow, the major component of the energy hub, the following subsection provides the functions used for objectives and constraints of optimization.

3.1. Objectives

In this research, two optimization objectives were considered. In the first objective, the cost of energy per day was kept to a minimum by applying different constraints including various demands on the hub output, price of the energy, the time window set by customers to schedule the use of electrical equipment, and constraints used for optimization (see Equation (1)). The energy cost minimized in the first objective refers to the costs related to buying electricity, gas, the absorption chiller, and the solar panels, as well as operational costs associated with storing electricity and heat. It is important to note that no investment cost was accounted for in the energy cost. The proposed hub will provide financial benefits as the upstream network provider will purchase the generated power.

$$Cost = \sum_{t=1}^{24} \left[\begin{array}{c} EPr(t).E^{buy-G}(t).\Delta t \\ +NGPr.E_g^{CHP}(t).\Delta t \\ \psi^{EES}.E^{EES}(t).\Delta t + \varphi^{TSS}.H^{TES}(t).\Delta t \\ +m^{chiller}.C_{CL}^{chiller}(t).\Delta t + m^{pv}.E^{pv}(t).\Delta t \\ -EPr(t).E^{sell-G}(t).\Delta t \end{array} \right] \quad (1)$$

where $EPr(t)$ is price of the energy tariff from the grid, $NGPr$ is the price of gas, $E^{sell-G}(t)$ and $E^{buy-G}(t)$ are the amount of energy sold and bought from the grid, $H^{TES}(t)$ is the

amount of heat, $m^{chiller}$ is the chiller maintenance cost, m^{pv} is the pv maintenance cost, $E^{pv}(t)$ is the energy of pv , and φ^{TSS} is the cost of heat utilization.

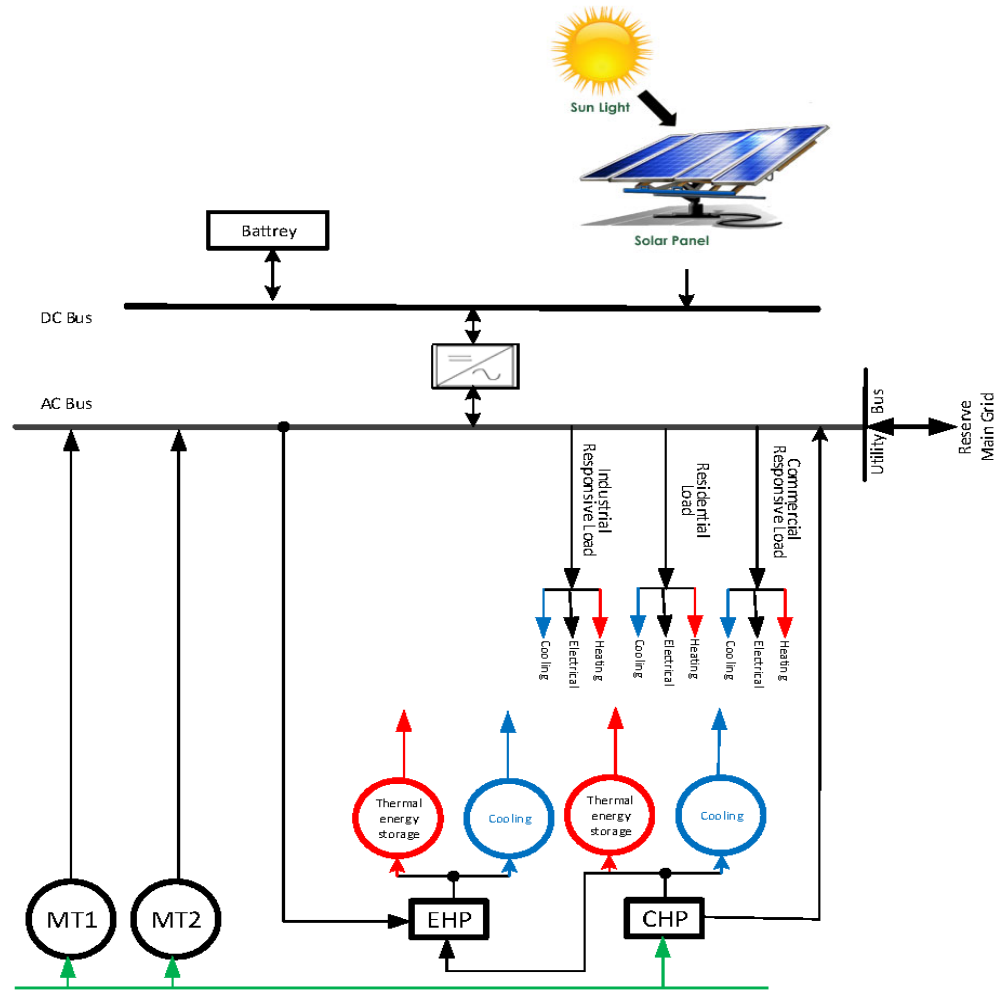


Figure 1. Proposed energy hub model and energy flow.

The second objective was to lower the emissions of CO₂ to a minimum level. Both the CHP unit and the commonly used (traditional) electrical grid produce the CO₂ emissions (see Equation (2)).

$$Emissions = \sum_{t=1}^{24} \left(\xi_{CO_2}^{CHP} \times E_g^{CHP}(t) \times \eta_e^{CHP} + \xi_{CO_2}^G(t) \cdot E^{buy-G}(t) \right) \cdot \Delta t \quad (2)$$

where $E_g^{CHP}(t)$ is electricity generated from CHP , η_e^{CHP} is CHP efficiency, $\xi_{CO_2}^G$ is the emission of the grid, and $\xi_{CO_2}^{CHP}$ is the emission of CHP .

The main aim of this study was concurrent minimization of both the energy cost and CO₂ emissions. Therefore, the first and second objectives are combined in a multi-objective formula (see Equation (3)).

$$F = Min_{x \in Q} \{Cost(x), Emissions(x)\} \quad (3)$$

where x refers to the decision variables vector and Q is defined as the viable solution space defined by taking all the problem constraints into consideration.

3.2. Energy Balance

The electricity produced in the CHP, the electricity received from the upstream network and solar panels, and the electricity released from electric storage equipment provided the complete supply for electricity demand (see Equation (4)).

$$EL(t) = E_{EL}^G(t) + (E_{EL}^{PV}(t) + E_{EL}^{EES}(t)) \cdot \eta_{DC-AC} + E_{EL}^{CHP}(t) \quad (4)$$

where $E_{EL}^G(t)$, $E_{EL}^{PV}(t)$, $E_{EL}^{EES}(t)$, $E_{EL}^{CHP}(t)$ are electricity energy from the grid, PV unit, battery and CHP, respectively.

The heat produced in the thermal modes of the CHP and EHP as well as the heat released from the thermal storage provided the complete supply for thermal demand (see Equation (5)).

$$TL(t) = H_{TL}^{TES}(t) + H_{TL}^{CHP}(t) + H_{TL}^{EHP}(t) \quad (5)$$

where $H_{TL}^{TES}(t)$, $H_{TL}^{CHP}(t)$, $H_{TL}^{EHP}(t)$ are heat delivered from the TES, CHP, and EHP respectively.

The cooling generated in the absorption chiller and cooling produced in the cooling mode of the EHP provided the complete supply for the cooling demand (see Equation (6)).

$$CL(t) = C_{CL}^{Chiller}(t) + C_{CL}^{EHP}(t), \quad (6)$$

where $C_{CL}^{Chiller}$ is cooling generated from the chiller and C_{CL}^{EHP} is cooling generated from the EHP.

3.3. CHP System Constraints

Gas was fed into the CHP unit which produced electricity and heat concurrently. This research adopted an electricity-based CHP. In this type of CHP, the amount of heat produced is predicated on electricity generation. It is important to note that there is a relation between the electricity and heat produced in a CHP unit. The heat/power ratio is always defined as a constant value [9]. Equations (7) and (8) define the electrical and thermal energy produced in a CHP unit, respectively [2]:

$$E^{CHP}(t) = E_g^{CHP}(t) \times \eta_e^{CHP} \quad \forall t \quad (7)$$

$$H^{CHP}(t) = E_g^{CHP}(t) \times \eta_H^{CHP} \quad \forall t \quad (8)$$

where E_g^{CHP} is energy generated from the CHP and H^{CHP} heat from the *chp*.

Additionally, the paths for dispatching electrical and thermal energy in a CHP system are defined in Equations (9) and (10), respectively:

$$E^{CHP}(t) = E_{EL}^{CHP}(t) + E_G^{CHP}(t) + E_{EHP}^{CHP}(t) + \frac{E_{EES}^{CHP}(t)}{\eta_{AC-DC}} \quad (9)$$

$$H^{CHP}(t) = H_{TL}^{CHP}(t) + H_{TES}^{CHP}(t) + H_{chiller}^{CHP}(t) \quad (10)$$

Each CHP unit has its own designed capacities which constrain the electrical and thermal outputs of the unit. These constraints for electrical and thermal outputs are defined in Equations (11) and (12), respectively [2]:

$$H^{EHP}(t) = [E_{EHP}^G(t) + E_{EHP}^{CHP}(t) + E_{EHP}^{EES}(t) \cdot \eta_{DC-AC}] \cdot COP_{EHP}^{Heating} \quad (11)$$

$$0 \leq H^{CHP}(t) \leq C_H^{CHP} \quad \forall t \quad (12)$$

where $COP_{EHP}^{Heating}$ is the performance coefficient of EHP.

3.4. EHP System Constraints

Electric heat pumps (EHP) are an effective and low-cost substitute for boilers. There are two modes in any EHP system: heating and cooling. These two modes cannot operate

at the same time. Equations (13)–(18) define the constraints associated with the EHP system. In these equations, $p(t)$ and $k(t)$ are binary variables used for preventing the concurrent occurrence of heating and cooling modes in the EHP system [14]:

$$H^{EHP}(t) = [E_{EHP}^G(t) + E_{EHP}^{CHP}(t) + E_{EHP}^{EES}(t) \cdot \eta_{DC-AC}] \cdot COP_{EHP}^{Heating} \forall t \quad (13)$$

$$H^{EHP}(t) = H_{TL}^{EHP}(t) + H_{TES}^{EHP}(t) \forall t \quad (14)$$

$$C_{CL}^{EHP}(t) = [E_{EHP}^G(t) + E_{EHP}^{CHP}(t) + E_{EHP}^{EES}(t) \cdot \eta_{DC-AC}] \cdot COP_{EHP}^{cooling} \forall t \quad (15)$$

$$C_{CL}^{\min,EHP} \cdot p(t) \leq C_{CL}^{EHP} \leq C_{CL}^{\max,EHP} \cdot p(t) \forall t \quad (16)$$

$$H^{\min,EHP} \cdot k(t) \leq H^{EHP}(t) \leq H^{\max,EHP} \cdot k(t) \forall t \quad (17)$$

$$p(t) + k(t) \leq 1 \forall t. \quad (18)$$

3.5. Absorption Chiller Constraints

The constraint of dispatching paths of the cooling energy is determined through Equation (19) while the constraint related to the cooling capacity of the absorption chiller is defined in Equation (19) [14]

$$C_{CL}^{chiller}(t) = (H_{chiller}^{CHP}(t) + H_{chiller}^{TES}(t)) \cdot COP^{chiller} \forall t \quad (19)$$

$$C_{CL}^{\min,chiller} \leq C_{CL}^{chiller}(t) \leq C_{CL}^{\max,chiller} \forall t \quad (20)$$

where $C_{CL}^{chiller}$ is the cooling capacity of the chiller, $H_{chiller}^{TES}$ is heat transferred from the heat storage to the chiller, and $H_{chiller}^{CHP}$ is heat transferred from the CHP to the chiller.

3.6. Electrical Energy Storage Constraints

The charge of, discharge of, and energy stored in an electrical storage are determined through Equations (21)–(23), respectively. Power produced from the CHP unit, supply from upstream electricity network, and the electricity output from solar panels can be used to charge the electricity energy storage (EES). In addition, EHP consumption, electrical load consumption, and sales to the upstream network can be provided by discharging power from the electricity storage.

$$E_{EES}(t) = ((E_{EES}^G(t) + E_{EES}^{CHP}(t)) \cdot \eta_{AC-DC} + E_{EES}^{pv}(t)) \cdot \eta_{EES}^{charge} \forall t \quad (21)$$

$$E^{EES}(t) = \frac{(E_G^{EES}(t) + E_{EL}^{EES}(t) + E_{EHP}^{EES}(t))}{\frac{\eta_{DC-AC}}{\eta_{EES}^{charge}}} \forall t \quad (22)$$

$$Eng^{EES}(t) = Eng^{EES}(t-1) + \Delta t \cdot E_{EES}(t) - \Delta t \cdot E^{EES}(t) \forall t \quad (23)$$

Equation (24) defines the rates for charging the EES, while discharging rates of the EES are determined in Equation (25):

$$0 \leq E_{EES}(t) \leq P^{\max,EES} \cdot r(t) \forall t \quad (24)$$

$$0 \leq E^{EES}(t) \leq P^{\max,EES} \cdot m(t) \forall t \quad (25)$$

The binary variables, namely $m(t)$ and $r(t)$, in Equation (26) guarantee that there is no simultaneous occurrence of charging and discharging of EES.

$$m(t) + r(t) \leq 1 \forall t \quad (26)$$

Equation (27) determines the minimum and maximum limits of the energy that is stored in the electrical storage [8]:

$$SOC_{EES}^{\min} \leq Eng^{EES}(t) \leq SOC_{EES}^{\max} \quad \forall t \quad (27)$$

In this study, the amount of energy stored in the electrical storage during the first hour of operation was specified as equal to the amount of energy stored in the last hour of operation. This raised the capacity of the storage device for subsequent days. This constraint is determined via Equation (28).

$$\sum_{t=1}^{24} (E_{EES}(t) - E^{EES}(t)) = 0 \quad \forall t \quad (28)$$

3.7. Thermal Energy Storage Constraints

The definition of thermal energy storage (TES) constraints are similar to the constraints that apply to the EES. Equations (29)–(36) determine the TES constraints. Two binary variables, namely $z(t)$ and $y(t)$, guarantee that there is no simultaneous occurrence of charging and discharging of TES.

$$H_{TES}(t) = (H_{TES}^{CHP}(t) + H_{TES}^{EHP}(t)) \cdot \eta_{TES}^{charge} \quad \forall t \quad (29)$$

$$H^{TES}(t) = \frac{(H_{TL}^{TES}(t) + H_{chiller}^{TES}(t))}{\eta_{TES}^{Discharge}} \quad \forall t \quad (30)$$

$$Eng^{TES}(t) = Eng^{TES}(t-1) + \Delta t \cdot H_{TES}(t) - \Delta t \cdot H^{TES}(t) \quad \forall t \quad (31)$$

$$0 \leq H_{TES}(t) \leq P^{\max, TES} \cdot y(t) \quad \forall t \quad (32)$$

$$0 \leq H^{TES}(t) \leq P^{\max, TES} \cdot z(t) \quad \forall t \quad (33)$$

$$z(t) + y(t) \leq 1 \quad \forall t \quad (34)$$

$$SCO_{TES}^{\min} \leq Eng^{TES}(t) \leq SOC_{TES}^{\max} \quad \forall t \quad (35)$$

$$\sum_{t=1}^{24} (H_{TES}(t) - H^{TES}(t)) = 0 \quad \forall t \quad (36)$$

3.8. Constraints Associated with Buying Electricity and Gas from the Upstream Network

Equation (37) specifies the electric power bought from the service provider of the upstream network. This electric power was utilized for electrical loads, electrical storage, and the EHP unit.

$$E^{buy-G}(t) = E_{EL}^G(t) + E_{EHP}^G(t) + E_{ESS}^G(t) / \eta_{AC-DC} \quad \forall t \quad (37)$$

In addition, the CHP unit and the discharge of the EES produced the electricity which could be purchased by the service provider of the upstream network. This constraint is determined through Equation (38):

$$E^{sell-G}(t) = E_G^{CHP}(t) + E_G^{EES}(t) \cdot \eta_{DC-AC} \quad \forall t \quad (38)$$

The line capacity is defined in Equations (39) and (40). Through the line, the electrical energy is exchanged with the grid over any time interval (t).

$$E^{sell-G}(t) \leq E^{G, \max} \cdot \tau(t) \quad \forall t \quad (39)$$

$$E^{buy-G}(t) \leq E^{G, \max} \cdot \ell(t) \quad \forall t \quad (40)$$

Equation (41) includes two binary variables, namely $m(t)$ and $n(t)$, used for preventing the concurrent sending and receiving of electrical energy from EDS.

$$\tau(t) + \ell(t) \leq 1 \quad \forall t \quad (41)$$

Equation (42) specifies the constraint associated with gas consumption in the CHP unit.

$$E_g^{CHP}(t) \leq E_g^{\max} \forall t \quad (42)$$

3.9. Demand Response Modeling

There are two types of electrical demands considered in the proposed energy hub: responsive and nonresponsive. Two categories of responsive demands were considered:

1. On/off responsive loads: The operation of these responsive loads can be in on/off mode. A typical example is the industrial load. The operation time in this type of load should be definitive in order to finish its task. The operation time needs to be within an acceptable time interval, which is specified by the consumers. Equation (43) defines this constraint for electrical loads [2].

$$\sum_{t=b_i^e}^{e_i^e} I_i^e(t) = U_i^e \forall i \quad (43)$$

Equation (44) determines the energy consumed in this category of responsive loads [2].

$$E_i(t) = E_i \cdot I_i^e(t) \forall i, t \quad (44)$$

2. Other responsive loads: Similar to on/off response loads, in other responsive loads the consumption level of energy, such as commercial load, is controllable. However, the hourly usage of energy in responsive commercial loads is limited to certain values. The technical settings of the loads and the consumer habit define the range of these values. A mathematical description of the value ranges for electrical loads is shown in Equation (45) [2]

$$E_j^{\min}(t) \leq E_j(t) \leq E_j^{\max}(t) \quad (45)$$

Equation (46) provides the mathematical formal for computing the daily energy consumption of load j :

$$\sum_t E_j(t) = E_j \forall j \quad (46)$$

According to the above-mentioned explanations, the following equation is derived.

$$\sum_i E_i(t) + \sum_j E_j(t) = EL^{res}(t) \quad (47)$$

3.10. Weighted Sum Approach

In the weighted sum approach, various weights were assigned to conflicting objective functions to obtain different Pareto optimal solutions. The trial assignment of different values to the weights helped with optimization and found acceptable solutions from the Pareto set. Equation (48) expresses the function for this multi-objective optimization problem using the weight sum approach [22]:

$$\min[\varpi] = \mathbb{N}_1 \varpi_1 + \mathbb{N}_2 \varpi_2 \quad (48)$$

where

$$\mathbb{N}_1 + \mathbb{N}_2 = 1 \quad (49)$$

The multi-objective optimization formulas typically included conflicting objective functions with various dimensions. Therefore, there was a need to transform the objective functions to per unit values based on the fuzzy satisfying approach. This is described in further details in the subsequent section.

3.11. Fuzzy Satisfying Approach

Various approaches were used for finding solutions to the multi-objective. As a result, many optimal solutions were found. Among these solutions, the best possible solution

enabled a win–win plan of action by taking all the conflicting objective functions into consideration. Firstly, all the objective functions were normalized. This stems from the fact that each objective function has its own dimension and value range. This was a multi-objective problem that aimed to minimize its objective functions. Through the use of fuzzy membership, the value of each objective function was transformed into the interval $[0, 1]$. Therefore, Equation (50) specifies the linear membership function for the solution of the objective function [23]:

$$\varpi_h^\Omega \leq \varpi_h^{Min} \quad \varpi_h^\Omega = \begin{cases} 1 \\ \frac{\varpi_h^\Omega - \varpi_h^{Max}}{\varpi_h^{Min} - \varpi_h^{Max}} \\ 0 \end{cases} \quad (50)$$

where ϖ_h^{Max} and ϖ_h^{Min} refer to the maximum and minimum values of the objective function k in the solutions found for the multi-objective problem. The optimality of the n -th solution for the k -th objective function was determined by ϖ_h^Ω . Equations (51) and (52) provide the normalization formulae for the two objective functions (i.e., minimizing energy cost and CO₂ emissions) defined in this study [16].

$$Cost_{pu} = \varpi_{1,pu} = \frac{Cost - Cost^{Max}}{Cost^{Min} - Cost^{Max}} \quad (51)$$

$$Emissions_{pu} = \varpi_{2,pu} = \frac{Emissions - Emissions^{Max}}{Emissions^{Min} - Emissions^{Max}} \quad (52)$$

The membership function for the n -th solution was computed through Equation (53) [16]

$$\Omega = 1, 2, \dots, \Theta \varpi^\Omega = \text{Min}(\varpi_1^\Omega, \dots, \varpi_\Theta^\Omega) \quad (53)$$

The maximum weakest membership function provided the most optimum solution for the multi-objective optimization problem [16].

$$\varpi^\Omega = \text{Max}(\varpi^1, \dots, \varpi^\Theta) \quad (54)$$

3.12. Point Estimation Method

The point estimation method was a significantly effective approach for studying power systems, compared to the other methods used for modelling uncertainty. This method decreased the computational content, accelerated the response speed, and provided a high degree of accuracy. This method of estimation concentrated the statistical information given in the early central moments of a problem and inputted random variable on K points for each variable. This is known as concentrations. Uncertainty information related to the output random variables of the problem were determined through the use of K points for each variable and the function F , which defined the relation between the input and output variables. The composition of a location $P_{l,k}$ and a weight $\omega_{l,k}$ provided the definition of the K th concentration $(P_{l,k}, \omega_{l,k})$ for a random variable P_L . The K th value of variable P_L was defined as the location $P_{l,k}$, in which the function F is assessed. The weight $\omega_{l,k}$ referred to a weighting factor that defined the relative significance of the assessment in the output random variables, using point estimation methods.

The assessment of function F must only be K times for each input random variable P_L , at the K points made up of the K th location $P_{l,k}$ of the input random variable P_L , and the mean (μ) of the $m - 1$ remaining input variables, i.e., at the K points $(\mu_{P1}, \mu_{P2}, \dots, P_{l,k}, \dots, \mu_{Pm})$. Therefore, there must be K solutions of the deterministic problem for each input random variable P_L . The deterministic value $P_{l,k}$ given to P_L provided the difference among these problems while fixing the remaining input random variables based on their mean values. The adopted scheme provided the basis for specifying the number of K evaluations. As a result, $K \times m$ defined the overall number of evaluations for the function F . One more assessment of the function F at a specific point, which is defined by

the m input random variables means $(\mu_{p,1}, \mu_{p,1}, \dots, \mu_{p,l}, \dots, \mu_{p,m})$, was considered in particular variants or schemes of the point estimation method. If there are too many input random variables, the result obtained from the two-estimation method is not satisfactory and it does not provide an acceptable solution for addressing the problems with a pragmatic scale in the power systems. To eliminate this impediment, the $2m + 1$ scheme should consider just one extra assessment for the function [24,25].

Equation (55) specifies the location $P_{l,k}$:

$$P_{l,k} = \mu_{pl} + \xi_{l,k} \sigma_{pl} \quad (55)$$

where $\xi_{l,k}$ refers to the standard location, and μ_{pl} and σ_{pl} (input data) defined the mean and standard deviation values for the input random variable P_l , respectively.

The solutions for Equations (56)–(58) provided the values of the standard location $\xi_{l,k}$ and the weight $\omega_{l,k}$:

$$\xi_{l,k} = \frac{\lambda_{l,3}}{2} + (-1)^{3-k} \sqrt{\lambda_{l,4} - \frac{3}{4} \lambda_{l,3}^2} \quad k = 1, 2 \quad \xi_{l,3} = 0 \quad (56)$$

$$\omega_{l,k} = \frac{(-1)^{3-k}}{\xi_{l,k}(\xi_{l,1} - \xi_{l,2})} \quad (57)$$

$$\omega_{l,3} = \frac{1}{m} - \frac{1}{\lambda_{l,4} - \lambda_{l,3}^2} \quad (58)$$

At each point $(\mu_{p1}, \mu_{p2}, \dots, P_{l,k}, \dots, \mu_{pm})$, deterministic optimization was executed. An optimization problem was solved through Equation (59)

$$Z(l, k) = F(\mu_{p1}, \mu_{p2}, \dots, P_{l,k}, \dots, \mu_{pm}) \quad (59)$$

In Equation (59), $Z(l, k)$ refers to the vector that included output random variables associated to the K th concentration of random variable P_l , and F defined the nonlinear relation between the input and output variables in the optimization problem. The concentration scheme provided the basis for the entire number of executing the deterministic optimization problem. The estimation of t and the raw moments of the output random variables was conducted using the vector $Z(l, k)$.

$$E(Z) \cong E(Z) + \omega_{l,k} Z(l, k) \quad (60)$$

$$E(Z^j) \cong E(Z^j) + \omega_{l,k} (Z(l, k))^j \quad (61)$$

The below flowchart (Figure 2) represents $2m + 1$ strategy.

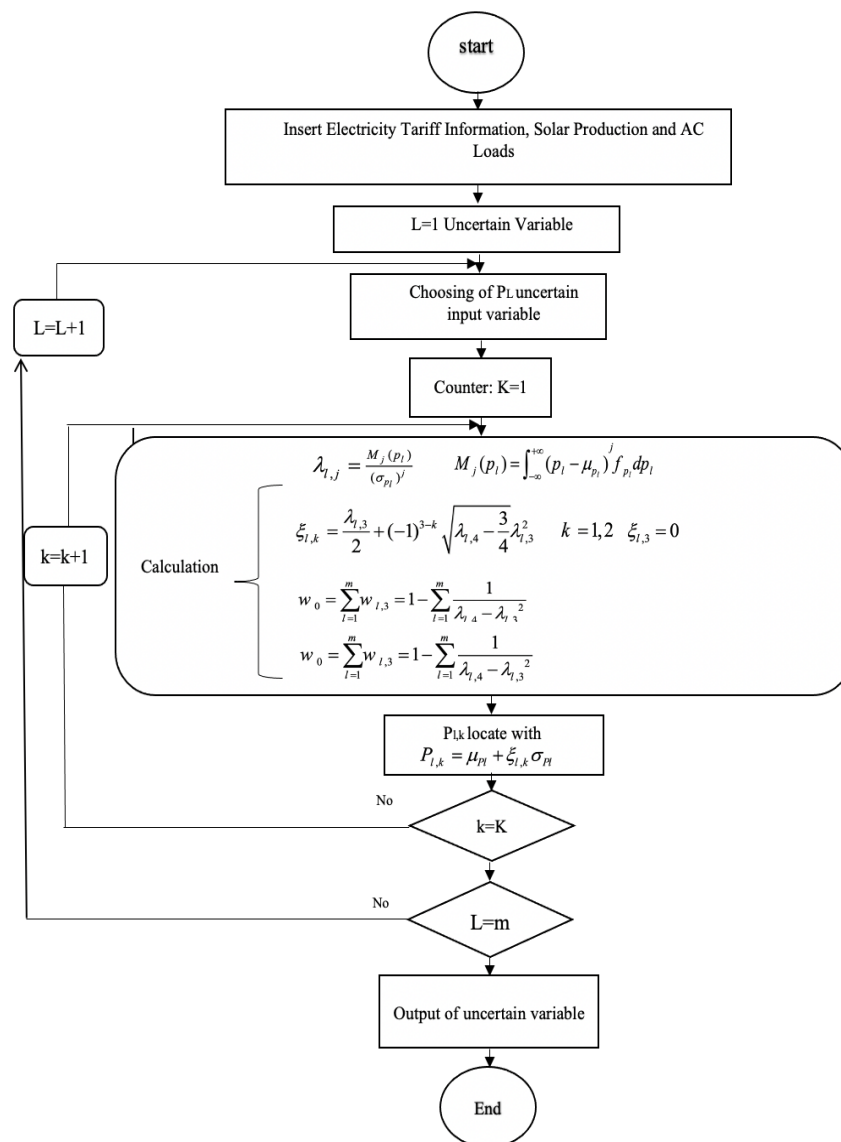


Figure 2. 2m + 1 strategy.

4. Numerical Results

This considered a hypothetical energy consumer for implementation of the proposed hub model. The schedule of the energy hub was based on different factors, namely, electricity tariff, CO₂ intensity, and the electricity task time window on both cold and hot days. This helped to explore the role that the EHP played in providing the consumer’s cooling and thermal load, as well as the impact of EHP on operating and scheduling the hub. The General Algebraic Modeling Software (GAMS) software package for optimization was used for implementing the mixed integer programming (MIP) model. The C programming language (CPLEX) program was used for solving the mixed integer programming (MIP) model.

4.1. Input Data

All parameters regarding commercial and residential loads were obtained from references [5,8]. Figure 3 shows the daily samples of AC and DC electricity loads in thermal and cooling energy hubs in two common scenarios: winter and summer. An assumption of our study was that price of the electricity was predicated on the time of use (TOU) approach. In addition, it was presumed that the rates for purchasing and selling the electricity were equal (see Figure 4a). The case study area was presumed to have the intensity profile of CO₂ in UK

on 17th of August in 2013. Figure 4b represents the intensity of CO₂ based on gCO₂/kWh electricity [26,27]. We also assumed that the cost of gas was 0.25 \$/KWh. Table 1 provides the adopted value for each parameter considered in the developed energy hub.

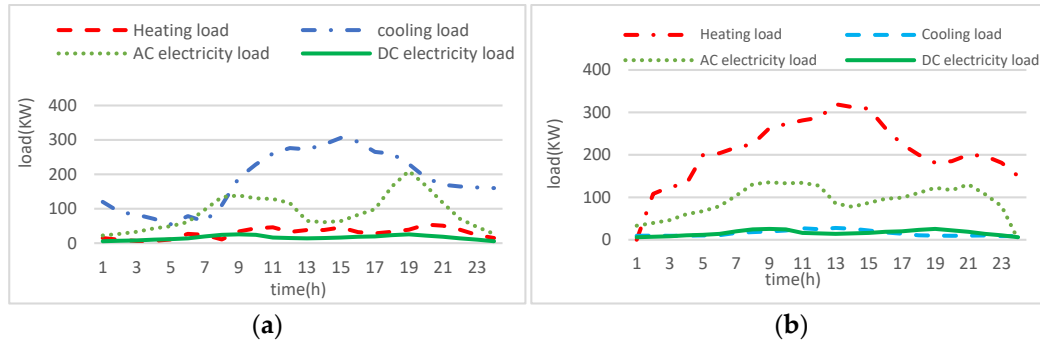


Figure 3. Electric, heating, and cooling loads: (a) sample winter day and (b) sample summer day.

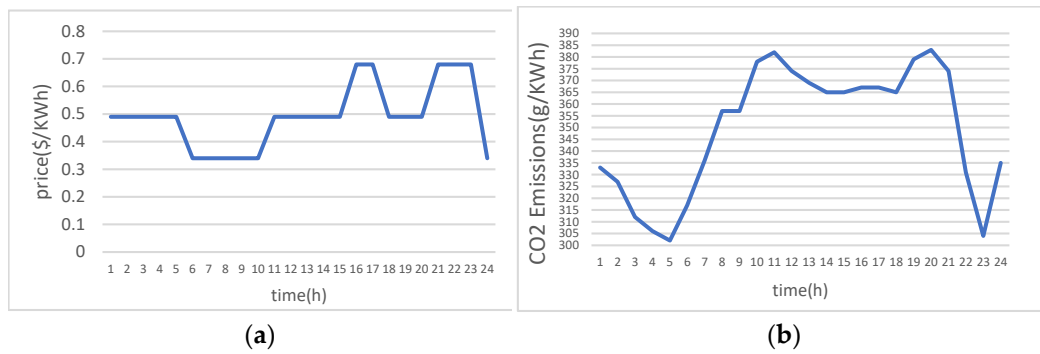


Figure 4. Electricity tariff (a) and CO₂ intensity (b).

Table 1. Proposed energy hub parameters.

Parameter	Value	Parameter	Value	Parameter	Value
η_e^{CHP}	0.4	$C^{max,EHp}$	450	$Eng^{TES(0)}$	1000
η_H^{CHP}	0.5	$C^{min,EHp}$	20	φ^{TSS}	0.009
C_E^{CHP}	150	COP^{ch}	0.75	$p^{max,EES}$	70
C_H^{CHP}	187.5	$C^{max,ch}$	300	SOC_{EES}^{max}	1000
$\xi_{CO_2}^{CHP}$	0.5	$C^{min,ch}$	0	SOC_{EES}^{min}	100
SC	0.54	$m^{chiller}$	0.02	η_{EES}^{charge}	0.87
SHC	0.54	η_{AC-DC}	0.87	$\eta_{EES}^{discharge}$	0.87
MUT	2	η_{DC-AC}	0.87	$Eng^{EES(0)}$	500
MDT	2	$p^{max, TES}$	150	ψ^{EES}	0.005
COP^H	2.5	SOC_{TES}^{max}	2000	m^{pv}	0.01
COP^C	2.5	SOC_{TES}^{min}	200	GLC	550
$H^{max,EHp}$	450	η_{TES}^{charge}	0.9	CLC	300
$H^{min,EHp}$	20	$\eta_{TES}^{discharge}$	0.9	NGPr	0.2

Another important assumption was that the proposed hub included industrial and commercial loads with controllable levels of hourly usage (consumption) in specified time intervals. Table 2 shows primary electricity tasks associated with each load. Subsequently, Tables 3 and 4 provide sample data describing the maximum and minimum limits of

energy consumption for industrial and commercial loads, respectively. In this context, the assumption was that industrial load consumed the overall electrical energy of 40 kWh diurnally, while the entire consumption of electrical energy in commercial loads was 30 kWh on each day.

Table 2. Electricity consumption tasks.

Task	Power (KW)	Earliest Starting Time (h)	Latest Finishing Time (h)	Time Window Length (h)	Energy Consumption (KWh)	Duration (h)
Industrial Loads	—	2	14	12	10	2
Commercial Loads	—	4	9	5	10	3

Table 3. A sample maximum and minimum allowable energy consumption for an industrial load.

Hours	[KWh] $E_1^{max}(t)$	[KWh] $E_1^{min}(t)$
1–7 and 18–24	8	0.1
8–17	10	0

Table 4. A sample maximum and minimum allowable energy consumption for a commercial load.

Hours	[KWh] $E_2^{max}(t)$	[KWh] $E_2^{min}(t)$
1–9 and 17–24	12	0
10–16	10	0.1

4.2. Deterministic Analysis

We presumed that the predicted values for the PV output power, the constant for AC electricity load, and the cost of energy were approximately the same as their real values when deterministic analysis of the proposed hub was performed [28]. Different scenarios were devised to examine different aspects of the proposed energy hub, namely, assessing the efficiency of all components of the hub, understanding the role of the EHP in providing heating and cooling loads, and evaluating the impact of the EHP on operating and scheduling the hub. The impact of selected (cold and hot) days in this study, as well as optimization functions on the hub equipment's efficiency, were considered as two important factors in the tested scenarios. The scenarios were:

Scenario 1: Operate the hub and minimize the electricity consumption cost during a sample winter day.

Scenario 2: Operate the hub and minimize the electricity consumption cost during a sample summer day.

Scenario 3: Operate the hub and minimize the electricity consumption cost and carbon footprint during a sample winter day.

Scenario 4: Operate the hub and minimize the electricity consumption cost and carbon footprint during a sample summer day.

The weighted sum method was adopted for solving the multi-objective model, which resulted in various solutions. All of these solutions were optimum; however, a promising solution in this study was the one that enabled a win–win plan of action by taking all the conflicting objective functions into consideration. This means that results from Scenarios 3 and 4 provide the most promising solution. Tables 5 and 6 respectively provide the solutions that we obtained for these scenarios.

Table 5. Pareto optimal solutions for scenario 3.

#	<i>N1</i>	<i>N2</i>	<i>Total Cost (kg)</i>	<i>CO₂ Emissions (kg)</i>	<i>1(pu)</i>	<i>2(pu)</i>	<i>min(Ø1 , Ø2)</i>
1	0	1	2054.95	1510.115	0	1	0
2	0.1	0.9	1917.418	1516.806	0.409	0.985	0.409
3	0.2	0.8	1895.245	1521.401	0.475	0.974	0.475
4	0.3	0.7	1846.32	1538.59	0.621	0.934	0.621
5	0.4	0.6	1829.67	1548.88	0.67	0.91	0.67
6	0.5	0.5	1793.59	1594.53	0.778	0.805	0.778
7	0.55	0.45	1787.074	1603.421	0.791	0.784	0.784
8	0.6	0.4	1785.911	1605.45	0.8	0.78	0.78
9	0.65	0.35	1769.65	1638.57	0.849	0.703	0.703
10	0.7	0.3	1769.15	1640.05	0.85	0.69	0.69
11	0.8	0.2	1741.06	1767.22	0.934	0.405	0.405
12	0.9	0.1	1719.09	1936.34	0.99	0.014	0.014
13	1	0	1718.83	1942.49	1	0	0

Table 6. Pareto optimal solutions for scenario 4.

#	<i>N1</i>	<i>N2</i>	<i>Total Cost (kg)</i>	<i>CO₂ Emissions (kg)</i>	<i>1(pu)</i>	<i>2(pu)</i>	<i>min(Ø1 , Ø2)</i>
1	0	1	1951.966	1493.538	0	1	0
2	0.1	0.9	1862.543	1508.185	0.574	0.962	0.574
3	0.2	0.8	1856.968	1510.276	0.61	0.956	0.61
4	0.3	0.7	1853.914	1512.701	0.63	0.95	0.63
5	0.4	0.6	1850.672	1517.36	0.65	0.938	0.65
6	0.5	0.5	1817.23	1575.54	0.865	0.786	0.786
7	0.6	0.4	1814.227	1583.58	0.884	0.765	0.765
8	0.7	0.3	1814.227	1583.58	0.884	0.765	0.765
9	0.8	0.2	1810.616	1618.043	0.908	0.675	0.675
10	0.9	0.1	1797.182	1821.287	0.994	0.146	0.146
11	1	0	1796.24	1851.023	1	0	0

The optimum solution for Scenario 3 is solution 7, which is chosen by applying the fuzzy satisfying approach (see Table 5). This solution has the maximum weakest membership function of 0.784. By choosing solution 7 in Scenario 3, the entire price of the system is \$1787.04, and the volume of CO₂ emissions is equal to 1603.421 kg. In addition, the optimum solution for Scenario 4 is solution 6, which is again chosen by applying the fuzzy satisfying approach (see Table 6). The solution has the maximum weakest membership function of 0.786. If solution 6 is selected in Scenario 4, the entire price of the system is \$1817.23, and the volume of CO₂ emissions is equal to 1575.54 kg. The major equipment of the energy hub is operated in each of the four scenarios defined in this study. Figure 5 represents these operations. In Scenario 1, during the hours 610 and 24, the cost of electricity is low, the mode of the EHP is set to heating, more heat is produced from the EHP, and the lowest amount of electricity and heat is produced. In addition, from the hour 11 to hour 15 the mode of the EHP is set to cooling due to high loads of cooling. The EHP fulfils the loads for cooling and there is no cooling generation in the chiller. In Scenario 2, the cooling load is higher than the heating load and, as a result, the mode of the EHP is only set to heating mode during the day except between the hours of 21 and 23. During these hours, there is a

high cost of electricity and therefore, the EHP generates cold. The entire capacity of the CHP unit is used for providing electricity during all hours except peak hours, namely, 6–10 and 24. This is because the cost of electricity is high during the peak hours.

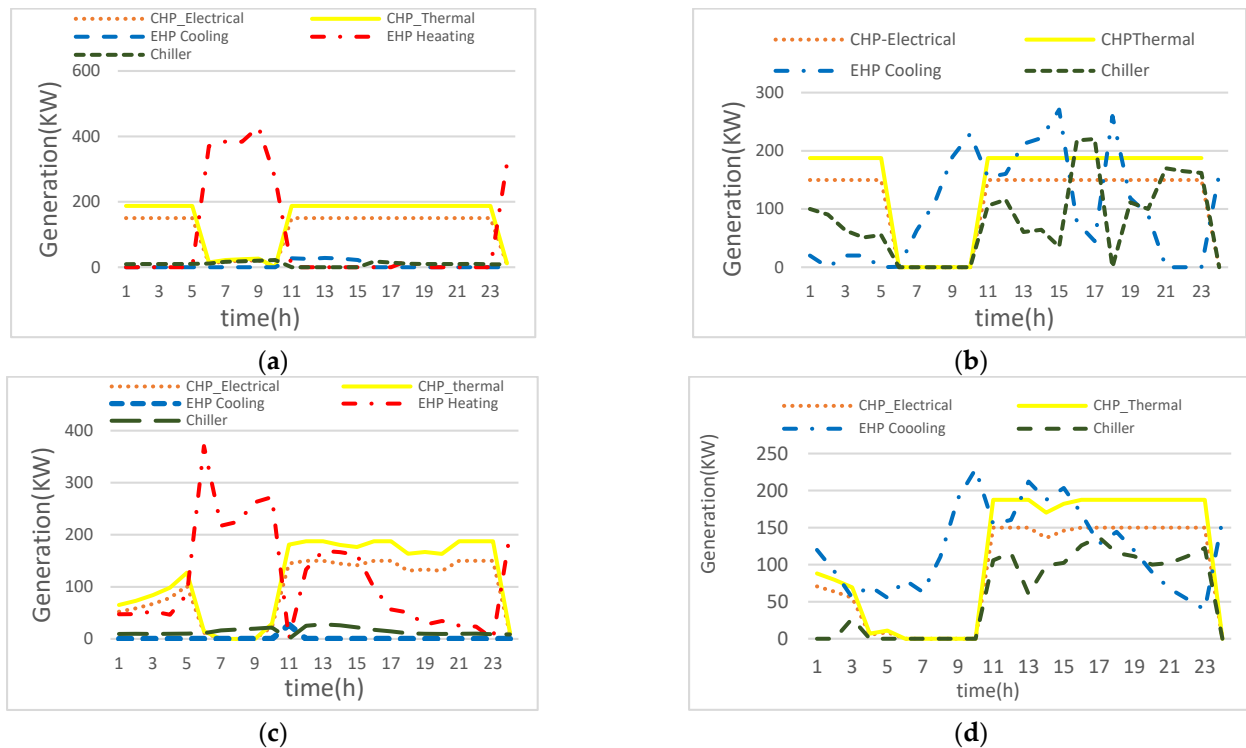


Figure 5. Operation of the main equipment. (a) scenario 1 (b) scenario 2 (c) scenario 3 (d) scenario 4.

The major hub equipment is operated in Scenario 3 by applying environmental and economic objectives. In Scenario 3, since CO₂ emitted from the CHP unit is higher than the upstream grid, there is an 18% reduction in electricity generation in comparison with Scenario 1. Additionally, there is a 26.1% rise in heat generation in comparison with Scenario 1. Therefore, the electricity sent to the EHP unit from the CHP unit is higher in Scenario 3 when we compare it with Scenario 1. Moreover, the AB chiller creates more cooling compared to Scenario 1. The primary preference for the EHP unit in Scenario 4 is supplying loads for cooling. As the load for cooling the building in this scenario is high, the operation of the EHP unit is based on the cooling mode. There is an increase of 15.25% in the heat produced through the EHP unit when we compare it with Scenario 2. To supply the electricity needed for operating the EHP unit in Scenario 4, 44.38% of the electricity is provided by the upstream grid and the remaining 55.62% is provided by the CHP unit. However, in Scenario 2, 61.7% of the electricity is provided by the upstream grid, and the remaining 38.3% is provided by the CHP unit. In addition, there is a reduction of 20.9% in the electricity produced in the CHP unit and a reduction of 23.85% in the cooling produced in the AB chiller compared to Scenario 2.

4.2.1. AC Electrical Load Balancing

By considering all four scenarios, the optimized strategies for supplying loads required for AC electricity, DC electricity, heating, and cooling are represented in Figures 6–9. Figure 6 indicates that the cost of electricity is high during 1 to 5 and 11 to 23 in Scenario 1. To supply the load required for electricity, the CHP unit should be operated. In addition, the upstream grid provides the maximum amount of electricity energy during the hours 6 to 10 and 24, when the cost of electricity is low.

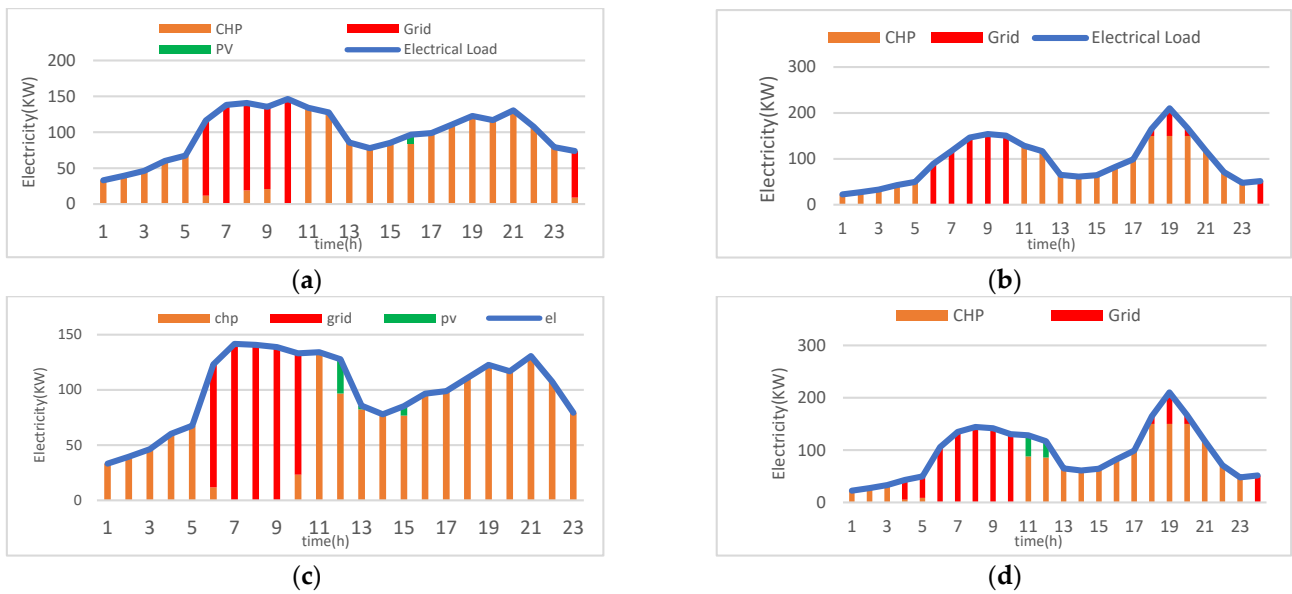


Figure 6. Optimal hourly AC-electrical demand balance (a) scenario 1 (b) scenario 2 (c) scenario 3 (d) scenario 4.

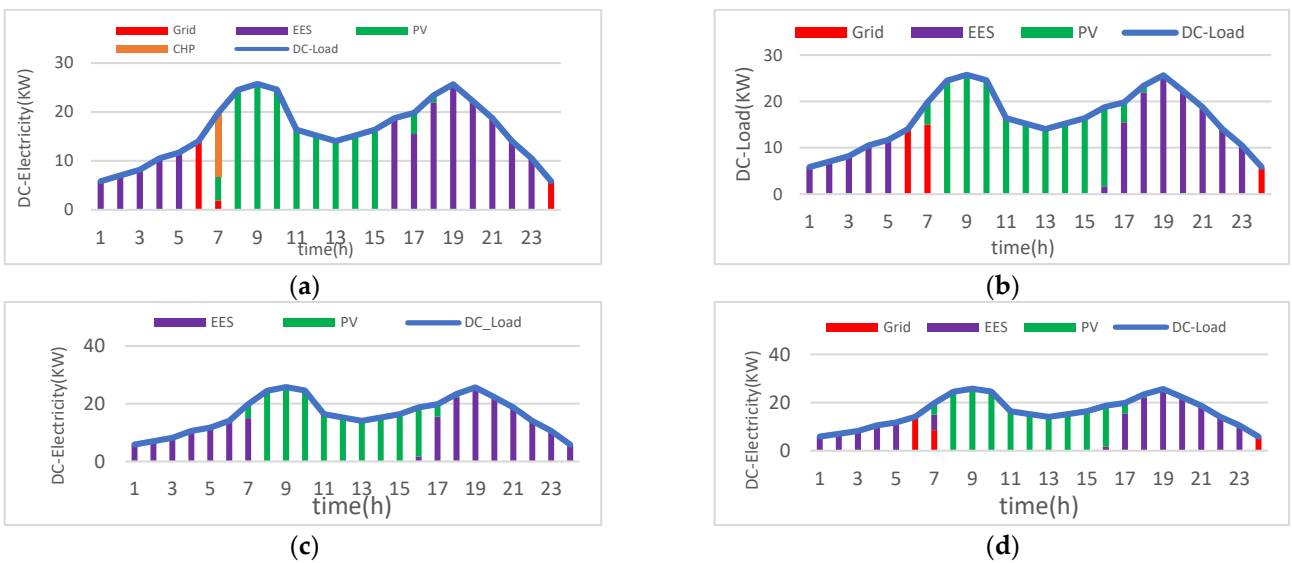


Figure 7. Optimal hourly DC-electrical demand balance (a) scenario 1 (b) scenario 2 (c) scenario 3 (d) scenario 4.

In the second Scenario, the provision of the loads for electricity is the responsibility of the CHP unit and the upstream grid. The CHP unit supplies the electricity load required in the hub during most hours, excluding the hours 6 to 10 and 24 when the cost of electricity is low. Furthermore, the load for AC electricity is provided by the cooperation of the upstream grid in two time periods when:

- The cost of electricity is low: This happens during the hours 6 to 10 and 24.
- The demand for AC electricity is higher than the capacity embedded in the CHP unit; it occurs during the hours 18 to 20.

By comparing Scenario 3 and Scenario 1, it is observed that the contribution of the CHP unit is reduced by 0.74% in Scenario 3. In addition, the contribution of the upstream grid in the hub has risen by 2.23%. Furthermore, the contribution of the PV unit has also increased in the third Scenario as we compare this scenario with the first Scenario.

The intensity of CO₂ in the 4th Scenario is higher than in the 2nd Scenario. Therefore, it is observed that the contribution of the CHP unit has reduced by 10.3% in Scenario 4. Additionally, the contribution of the upstream grid has risen by 8.9%.

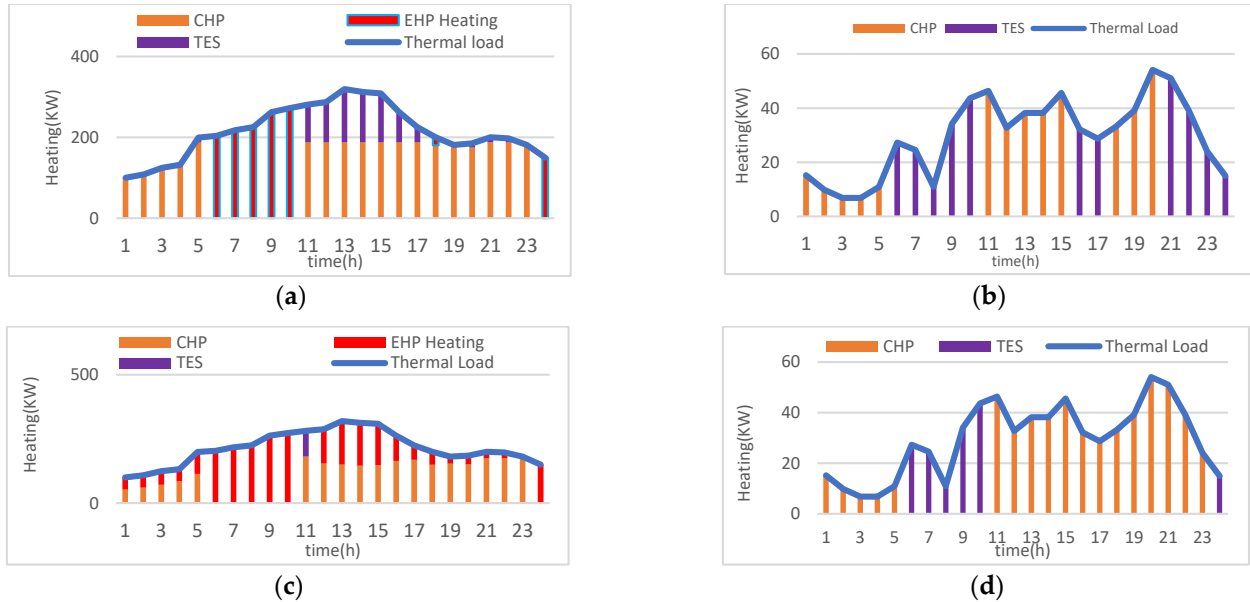


Figure 8. Optimal hourly heating demand balance (a) scenario 1 (b) scenario 2 (c) scenario 3 (d) scenario 4.

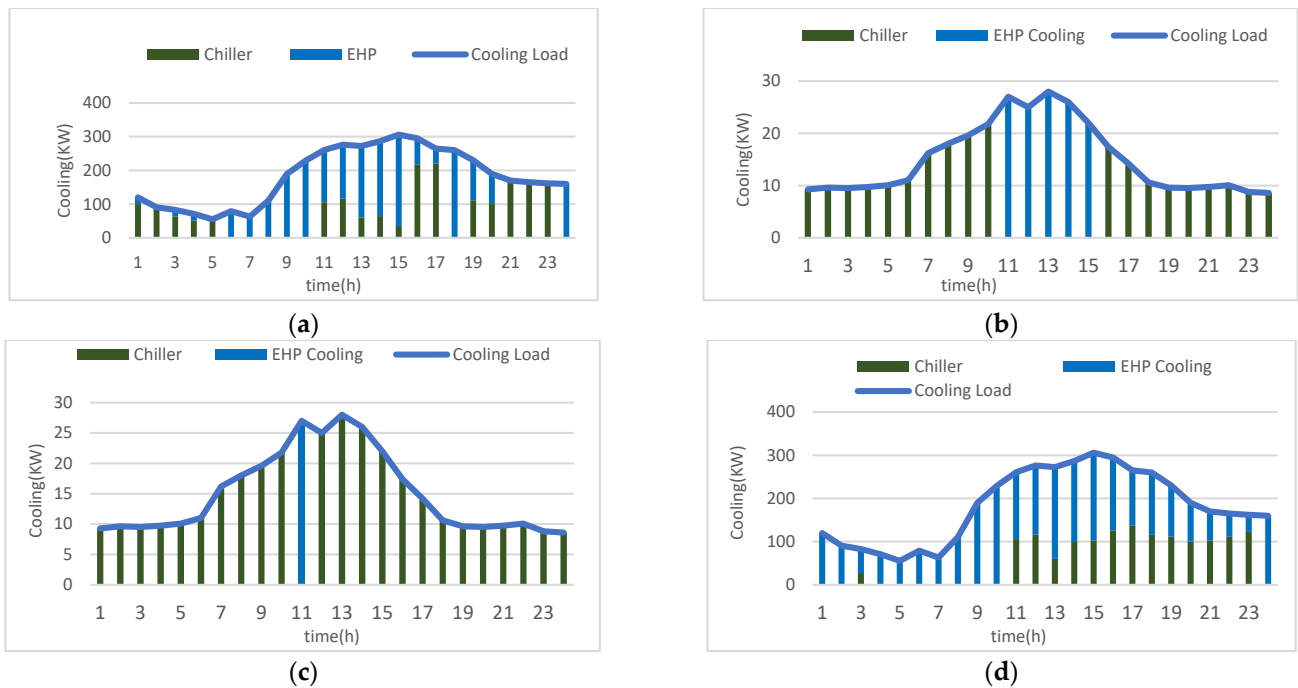


Figure 9. Optimal hourly Cooling demand balance (a) scenario 1 (b) scenario 2 (c) scenario 3 (d) scenario 4.

4.2.2. DC Electrical Load Balancing

Figure 7 indicates that the PV unit provides most of the load required for DC electricity in the energy hub during the hours 7 to 17 when the solar panels located on the rooftop provide the output power. In addition, the cooperation between the EES and the upstream grid is required for providing the load for DC electricity during the hours 1 to 6 and 18 to

24. When the output power provided by the solar panels is more than the demand needed for DC electricity, the remaining power is used for charging the electrical storage. However, if there is no output power provided by the solar panels, a release of electricity happens. In the 2nd Scenario, the contribution of both the PV unit and the upstream grid in providing the essential load for DC electricity of the hub has risen compared to Scenario 1. In the 3rd Scenario, the provision of the loads for DC electricity is the responsibility of the EES and the CHP unit. In this scenario, there is no cooperation between the CHP unit and the upstream grid to provide the loads for DC electricity. This is because of the CO₂ intensity of the upstream grid and the CHP unit.

In the 4th Scenario, the EES, PV unit, and upstream grid are responsible for supplying power for the loads. In comparison with the 2nd Scenario, there is a reduction in the contribution of the upstream grid while the contribution of the EES has risen.

The EES, PV unit, and upstream grid are responsible for supplying power for the loads.

4.2.3. Thermal Load Balancing

In the 1st Scenario, Figure 8a shows that the provision of the loads for heating is the responsibility of the EHP, CHP unit, and TES. The primary and secondary providers for the essential heating of the hub are the CHP and EHP, respectively. The EHP provides the entire thermal load during those hours that the cost of electricity is low, i.e., from 6 to 10 and 24. During other hours (i.e., 1 to 5 and 11 to 23), the TES and CHP provide the thermal load of the hub.

Figure 8b shows the 2nd Scenario, in which supplying the load for heating is the responsibility of the CHP unit and TES. The CHP unit provides the entire thermal load of the hub over three time periods, namely, 1 to 5, 11 to 15, and 18 to 20. During other time periods, supplying the thermal loads is the responsibility of the TES.

As depicted in Figure 8c, in the 3rd Scenario the essential heating of the hub is primarily provided by the EHP while the secondary supplier is the CHP unit; this contrasts with the 1st Scenario. In Scenario 3, the EHP and CHP provide 49.78% and 48.16% of the essential heating of the hub, respectively. The remaining 2.06% is provided by the TES. However, in the 1st Scenario, the EHP and CHP provide 26.3% and 59.5% of the heating needed in the hub, respectively. The TES provides the remaining 14.2%.

In the 4th Scenario, supplying the load for heating is the responsibility of the CHP and TES. The CHP unit provides the entire thermal load over those time periods when the cost of electricity is high, i.e., 1 to 5 and 11 to 23. During other hours, namely 6 to 10 and 24, the TES provides the required thermal load of the hub.

4.2.4. Cooling Load Balancing

In the 1st Scenario, as shown in Figure 9a, the essential cooling energy of the hub is primarily provided by the AB chiller while the secondary provider is the EHP. When the energy cost is middling, the demand for cooling is at maximum level, the mode of the EHP is set to cooling, and the CHP and TES provide the load for the heating of the hub. In the 2nd Scenario, the essential cooling energy of the hub is primarily provided by the EHP while the secondary provider is the AB chiller (see Figure 9b). The heating load is provided by the EHP during most hours, except those time intervals when the energy cost is at middle and high levels. The essential cooling energy of the hub is primarily provided by the AB chiller while the secondary provider is the EHP. The outcome shows that the EHP provides 7.47% of the essential cooling of the hub while the AB chiller provides the main 92.52%. In the 1st Scenario, the EHP provides 35.42% of the essential cooling of the hub and the AB chiller provides 64.58%. The essential cooling energy of the hub is primarily provided by the EHP while the secondary provider is the AB chiller. Compared to the 2nd scenario, the cooling produced from the EHP has risen by 15.25% while there is a reduction of 23.86% in the cooling produced from the AB chiller.

4.2.5. Exchange with Upstream Grid

Figure 10 represents the interplay between the electrical energy and the upstream grid in all the scenarios tested in this study. In the 1st Scenario, purchase of the electricity from the grid is mostly over the low-price time period, namely the hours 6 to 10. Moreover, the energy is mostly sold during the hours 1 to 5 and 11 to 23, which are the hours with high prices. In the 2nd Scenario, purchase of the electricity from the grid is mostly over three time periods, namely:

- From 6 to 10: In this time period, the cost of electricity is low.
- From 18 to 20: The capacity for producing electricity from the CHP provides a high load for ARC electricity during these hours.
- From 11 to 12: During this period, the cooling load is high and there is a need for EHP production.

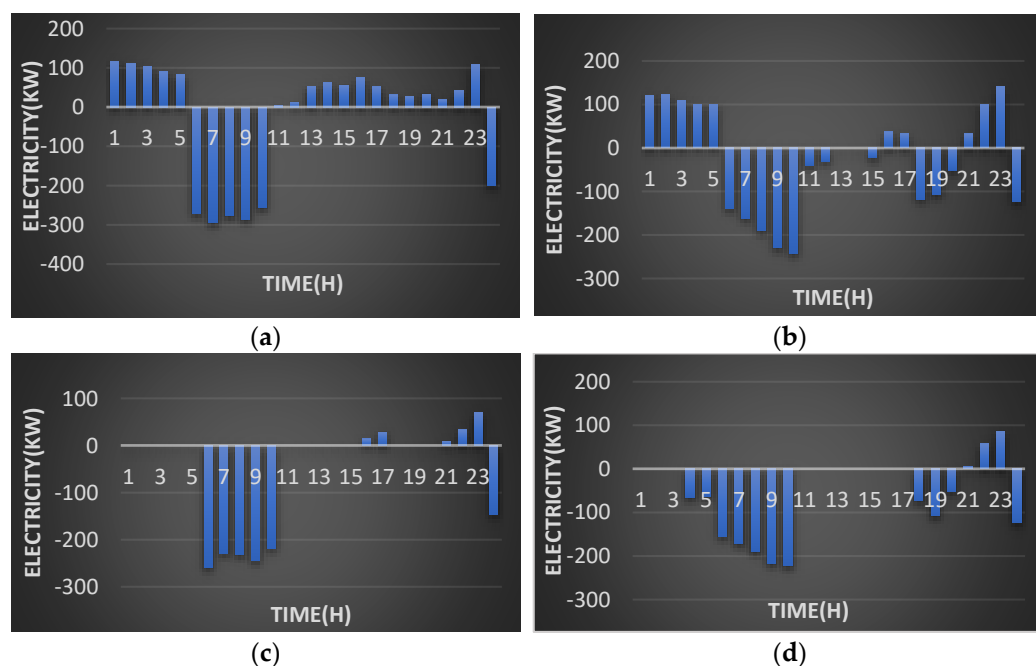


Figure 10. Optimal exchange power with grid, negative (purchasing) and positive (selling). (a) scenario 1 (b) scenario 2 (c) scenario 3 (d) scenario 4.

In addition, the electrical energy is sold during the hours with high prices in Scenario 2. In the 3rd Scenario, there is less interaction between the electrical energy and the upstream grid when we compare this scenario with the 1st Scenario. The outcomes in Scenario 3 show that there has been a reduction of 16% in the energy bought from the upstream grid and the sale of energy to the upstream grid is reduced by 85.5% compared to the 1st Scenario. In Scenario 3, exchanging the energy power with the upstream grid has been optimized in order to compromise between CO₂ intensity and electricity costs. Likewise, in Scenario 4, a compromise between CO₂ intensity and electricity costs is considered by optimization of the energy power exchanged with the upstream grid. There has been a reduction of 1.5% in purchasing energy from the upstream grid and the sale of energy to the upstream grid has reduced by 83.35% compared to Scenario 3.

4.2.6. Evaluation of Energy-Consuming Consumer Tasks

Figure 11 represents the entire usage of controllable loads of the energy for each scenario considered in this study. The usage of controllable loads in Scenarios 1 and 2 is at maximum level during the hours 6 to 10 and 24 when the electricity is low cost. Considering Scenarios 3 and 4, the usage of controllable loads is at maximum level between the hours 6 to 8 and 24, when energy is low cost, and the intensity of CO₂ is minimum. Figure 12

provides the entire costs and emitted CO₂ in each scenario. As illustrated in this figure, if the energy hub is operated by considering both electricity cost and CO₂ intensity, it will lead to higher costs and less CO₂ emission compared to operation of the hub by considering only the price of electricity.

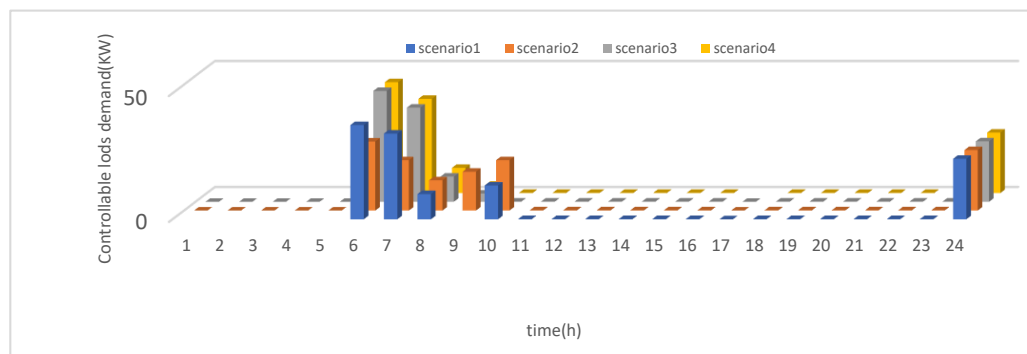


Figure 11. Controllable loads demand for all scenarios.

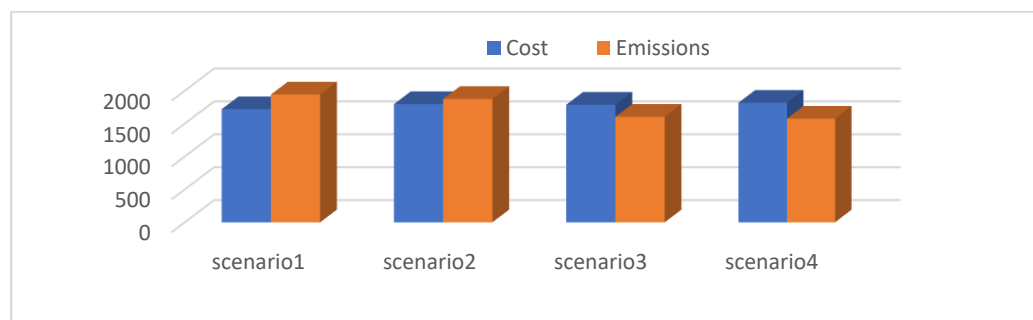


Figure 12. Cost and emissions for all scenarios.

4.3. Probabilistic Analysis

In the proposed energy hub, uncertainties associated with the load for AC electricity, cost of energy, and the power sourced from rooftop solar panels are modelled by applying the $2m + 1$ approach.

Since there are three uncertain variables, i.e., $m = 3$, seven solutions ($2m + 1 = 7$) should be obtained for the problem of managing energy. The efficiency of the $2m + 1$ approach is demonstrated by performing probabilistic optimization with the objective of minimizing the cost during an example day in the winter season. Table 7 provides the values for the expected optimum operation point of energy hub equipment, and the optimum exchange of power with the upstream grid and purchased energy. A comparison between these values and the values acquired from the deterministic approach is shown in Table 8. For instance, it is expected that the operation of the energy hub is priced at \$1801.9 in probabilistic analysis, whereas the value of this variable is projected to be \$1718.8 when using deterministic analysis. This indicates that if uncertainty is considered in operating the energy hub, there is a rise of 6.4% in the expected value for objective function. Moreover, as described in Tables 7 and 8, efficiency of the $2m + 1$ approach at an acceptable level is verified for operating the proposed hub using probabilistic analysis.

Table 7. Expected operation of energy hub evaluated using 2m + 1 method.

<i>TIME(t)</i>	<i>CHP_E</i>	<i>TES</i>	<i>EHP_H</i>	<i>EHP_C</i>	<i>Chiller</i>	<i>EES</i>	<i>GAS</i>	<i>Grid</i>
1	135.46	-51.25	0	0	9.28	6.72	338.65	103.02
2	137.1	-45.39	0	0	9.62	8.06	342.77	97.96
3	140.22	-34.41	0	0	9.5	9.41	350.55	93.88
4	141.73	-29.08	0	0	9.74	3.15	354.33	71.56
5	149.98	-11.74	35.88	0	10.08	13.44	374.96	68.71
6	11.74	-150	370.41	0	11	-13.12	29.35	-291.06
7	17.27	-146.06	379.79	0	16.19	2.87	43.17	-296.14
8	19.2	-130.02	369.51	0	18	-0.21	48	-300
9	25.66	-139.99	410.72	0	19.6	-18.29	64.17	-297.66
10	12.33	-35.37	328.61	0	21.76	-35.03	30.83	-287.33
11	149.98	104.15	0	26.99	0	-6.25	374.96	15.6
12	149.98	111.09	0	24.99	0	-19.08	374.96	25.33
13	150	146.52	0	28	0	-23.18	375	69.92
14	149.97	138.86	0	25.99	0	-27.32	374.92	75.84
15	150	134.72	0	22	0	11.04	375	93.75
16	149.97	109.08	0	0	17.39	0.33	374.92	58.83
17	149.98	62.69	0	0	14.19	1.95	374.96	43.63
18	149.98	6.26	20.98	0	10.59	8.35	374.96	7.07
19	149.98	7.31	0	0	9.62	14.42	374.96	-0.23
20	149.98	11.31	0	0	9.5	5.25	374.96	24.5
21	150	28.32	0	0	9.74	5.21	375	27.94
22	149.98	26.05	0	0	10.08	16.13	374.96	46.65
23	150	6.09	0	0	8.8	12.1	375	61.76
24	9.17	-131.06	295.63	0	8.6	-64.64	22.93	-300

Table 8. Operation energy hub for deterministic framework.

<i>TIME(t)</i>	<i>CHP_E</i>	<i>TES</i>	<i>EHP_H</i>	<i>EHP_C</i>	<i>Chiller</i>	<i>EES</i>	<i>GAS</i>	<i>Grid</i>
1	150	-67.61	0	0	9.28	6.72	375	116.78
2	150	-59.88	0	0	9.62	8.06	375	110.5
3	150	-45.4	0	0	9.51	9.41	375	103.73
4	150	-38.37	0	0	9.74	12.1	375	89.84
5	150	28.13	0	0	10.08	13.44	375	82.43
6	11.74	-150	370.41	0	11	0	29.35	-275.39
7	17.27	-150	384.16	0	16.19	0	43.14	-294.39
8	19.2	-142	383.66	0	18	-12.3	48	-275
9	20.9	-150	429.16	0	19.6	-31.26	52.26	-12/286
10	0	32.24	272.5	0	21.76	-42.09	375	-36/255
11	150	104.14	0	-27	0	-53.4	0	5.07
12	150	111.11	0	-25	0	-54.62	375	12.33

Table 8. *Cont.*

<i>TIME(t)</i>	<i>CHP_E</i>	<i>TES</i>	<i>EHP_H</i>	<i>EHP_C</i>	<i>Chiller</i>	<i>EES</i>	<i>GAS</i>	<i>Grid</i>
13	150	146.52	0	−28	0	−50.21	375	53.1
14	150	138.88	0	−26	0	−33.32	375	61.75
15	150	134.72	0	−22	0	−11.84	375	55.93
16	150	109.11	0	0	17.4	33.58	375	74.28
17	150	62.7	0	0	14.2	17.8	375	51.06
18	150	7.37	20	0	10.6	25.24	375	31.32
19	150	7.31	0	0	9.62	29.48	375	27.4
20	150	11.31	0	0	9.51	25.56	375	33.13
21	150	28.32	0	0	9.74	21.51	375	19.45
22	150	26.05	0	0	10.08	16.13	375	42.49
23	150	6.09	0	0	8.8	70	375	108.79
24	9.17	−150	316.33	0	8.6	0	22.93	−195.22

5. Conclusions

In this research, a probabilistic optimization method was utilized for developing a microgrid energy hub by considering the flow of energy between the hub components. In order to program and operate the energy hub, as well as usage in commercial and industrial electrical load tasks, this study suggested a MIP model. The weighted sum approach was used for optimizing both environmental and economic objectives. Besides, a comprehensive analysis was done to identify the role of the EHP in providing loads for both heating and cooling, as well as its impact on the costs, fuel usage, and electrical energy consumption in the proposed hub. This research adopted 2 m + 1 approach for managing all the uncertainties related to cost of electricity, the load for AC electricity, and the power sourced from rooftop solar panels.

According to numerical findings, during an example day in the winter season, if decreasing the price of energy is the goal for using the hub, the CHP unit is the primary provider of the heating loads while the EHP is the secondary provider. However, if we consider both environmental and economic objectives, the EHP is the major provider of the heating loads, and the CHP is the secondary provider.

During an example day in the summer season, if decreasing the price of energy is the goal for using the hub, the EHP is the primary provider of the cooling loads while the AB chiller is the secondary provider. However, if we consider both environmental and economic objectives, the contribution of the EHP in providing the cooling loads also rises. Therefore, a key approach for reducing the usage of energy and greenhouse gas emissions is based on electrification of heating and cooling. Moreover, the numerical findings indicate that if we consider the impact of uncertainty, objective function values rise, and this leads to the increase in the entire estimated prices.

Author Contributions: Conceptualization, H.R., S.M.M.T., M.H.A., A.Z.K. and S.K.; simulation and validation: H.R.; Writing, H.R.; supervision, S.M.M.T., A.Z.K. and S.K. All authors have read and agreed to the published version of the manuscript.

Funding: This research received no external funding.

Conflicts of Interest: The authors declare no conflict of interest.

References

1. Zhang, D.; Evangelisti, S.; Lettieri, P.; Papageorgiou, L.G. Economic and environmental scheduling of smart homes with micro grid: DER operation and electrical tasks. *Energy Convers. Manag.* **2016**, *110*, 113–124. [[CrossRef](#)]
2. Rastegar, M.; Fotuhi-Firuzabad, M.; Lehtonen, M. Home load management in a residential energy hub. *Electr. Power Syst. Res.* **2015**, *119*, 322–328. [[CrossRef](#)]
3. Khayyam, H.; Ranjbarzadeh, H.; Marano, V. Intelligent control of vehicle to grid power. *J. Power Sources* **2012**, *201*, 1–9. [[CrossRef](#)]
4. Sadeghi, M.; Mollahasani, S.; Erol-Kantarci, M. Cost-Optimized Microgrid Coalitions Using Bayesian Reinforcement Learning. *Energies* **2021**, *14*, 7481. [[CrossRef](#)]
5. Al-Saadi, M.; Al-Greer, M.; Short, M. Strategies for Controlling Microgrid Networks with Energy Storage Systems: A Review. *Energies* **2021**, *14*, 7234. [[CrossRef](#)]
6. Khayyam, H.; Abawajy, J.; Javadi, B.; Goscinski, A.; Stojcevski, A.; Stojcevski, A.; Bab-Hadiashar, A. Intelligent battery energy management and control for vehicle-to-grid via cloud computing network. *Appl. Energy* **2013**, *111*, 971–981. [[CrossRef](#)]
7. Tafreshi, S.M.M.; Ranjbarzadeh, H.; Jafari, M.; Khayyam, H. A probabilistic unit commitment model for optimal operation of plug-in electric vehicles in microgrid. *Renew. Sustain. Energy Rev.* **2016**, *66*, 934–947. [[CrossRef](#)]
8. Iman, G.M.; Mohsen, S.; Elaheh, M. Mprovement of energy performance employing electrical heat pump in scheduling a residential energy hub. *Int. Trans. Electr. Energy Syst.* **2016**, *26*, 2618–2642.
9. Rastegar, M.; Fotuhi-Firuzabad, M.; Zareipour, H.; Moeini-Aghtaie, M. A Probabilistic Energy Management Scheme for Renewable-Based Residential Energy Hubs. *IEEE Trans. Smart Grid* **2016**, *8*, 2217–2227. [[CrossRef](#)]
10. Pazouki, S.; Haghifam, M.-R.; Moser, A. Uncertainty modeling in optimal operation of energy hub in presence of wind, storage and demand response. *Int. J. Electr. Power Energy Syst.* **2014**, *61*, 335–345. [[CrossRef](#)]
11. Pazouki, S.; Haghifam, M.R.; Pazouki, S. Short term economical scheduling in an energy hub by renewable and demand response. In Proceedings of the 2013 3rd International Conference on Electric Power and Energy Conversion Systems, Istanbul, Turkey, 2–4 October 2013; pp. 1–6.
12. Shirazi, E.; Zakariazadeh, A.; Jadid, S. Optimal joint scheduling of electrical and thermal appliances in a smart home environment. *Energy Convers. Manag.* **2015**, *106*, 181–193. [[CrossRef](#)]
13. Ahmadi, S.E.; Rezaei, N.; Khayyam, H. Energy management system of networked microgrids through optimal reliability-oriented day-ahead self-healing scheduling. *Sustain. Energy Grids Netw.* **2020**, *23*, 100387. [[CrossRef](#)]
14. Moghaddam, I.G.; Saniei, M.; Mashhour, E. A comprehensive model for self-scheduling an energy hub to supply cooling, heating and electrical demands of a building. *Energy* **2016**, *94*, 157–170. [[CrossRef](#)]
15. Orehoung, K.; Evins, R.; Dorer, V. Integration of decentralized energy systems in neighborhoods using the energy hub approach. *Appl. Energy* **2015**, *154*, 277–289. [[CrossRef](#)]
16. Maroufmashat, A.; Elkamel, A.; Fowler, M.; Sattari, S.; Roshandel, R.; Hajimiragha, A.; Walker, S.; Entchev, E. Modeling and optimization of a network of energy hubs to improve economic and emission considerations. *Energy* **2015**, *93*, 2546–2558. [[CrossRef](#)]
17. Rastegar, M.; Fotuhi-Firuzabad, M.; Aminifar, F. Load commitment in a smart home. *Appl. Energy* **2012**, *96*, 45–54. [[CrossRef](#)]
18. Kamyab, F.; Bahrami, S. Efficient operation of energy hubs in time-of-use and dynamic pricing electricity markets. *Energy* **2016**, *106*, 343–355. [[CrossRef](#)]
19. Nazar Setayesh, M.; Haghifam, M.R. Multi objective electric distribution system expansion planning using hybrid energy hub concept. *Electr. Power Syst. Res.* **2009**, *79*, 899–911. [[CrossRef](#)]
20. Najafi, A.; Falaghi, H.; Contreras, J.; Ramezani, M. Medium-term energy hub management subject to electricity price and wind uncertainty. *Appl. Energy* **2016**, *168*, 418–433. [[CrossRef](#)]
21. Scala, L.; Vaccaro, A.; Zobaa, A. A goal programming methodology for multi objective optimization of distributed energy hubs operation. *Appl. Therm. Eng.* **2014**, *71*, 658–666. [[CrossRef](#)]
22. Majidi, M.; Nojavan, S.; Esfetanaj, N.N.; Najafi-Ghalelou, A.; Zare, K. A multi-objective model for optimal operation of a battery/PV/fuel cell/grid hybrid energy system using weighted sum technique and fuzzy satisfying approach considering responsible load management. *Sol. Energy* **2017**, *144*, 79–89. [[CrossRef](#)]
23. Brooke, A.; Kendrick, D.; Meeraus, A.; Raman, R. *GAMS A User's Guide*; GAMS Development Corporation: Washington, DC, USA, 2003.
24. Aien, M.; Fotuhi-Firuzabad, M.; Rashidinejad, M. Probabilistic Optimal Power Flow in Correlated Hybrid Wind–Photovoltaic Power Systems. *IEEE Trans. Smart Grid* **2014**, *5*, 130–138. [[CrossRef](#)]
25. Morales, J.M.; Perez-Ruiz, J. Point Estimate Schemes to Solve the Probabilistic Power Flow. *IEEE Trans. Power Syst.* **2007**, *22*, 1594–1601. [[CrossRef](#)]
26. A Note on Variations in UK/GB Grid Electricity CO₂ Intensity with Time—Earth Notes. 2015. Available online: <https://www.earth.org.uk/note-on-UK-grid-CO2-intensity-variations-by-year.html#fullyear2015> (accessed on 2 June 2021).
27. Combining Opzportunities with Markets. 2017. Available online: <http://www.ote-cr.cz/short-term-markets/electricity/day-ahead-market> (accessed on 2 June 2021).
28. PV Output. 2017. Available online: <https://pvoutput.org/live.jsp> (accessed on 2 June 2021).